Mat. Res. Soc. Symp. Proc. Vol. 690 © 2002 Materials Research Society

Circular Photogalvanic Effect in SiGe Semiconductor Quantum Wells.

Sergey D. Ganichev[1,2], Franz-Peter Kalz[1], Ulrich Rössler[1], Wilhelm Prettl[1],
Eugenius L. Ivchenko[2], Vasily V. Bel'kov[2], Robert Neumann[3], Karl Brunner[3], and Gerhard Abstreiter[3]
[1] Fakultät für Physik, Universität Regensburg, 93040 Regensburg, Germany,
[2] A. F. Ioffe Physico-Technical Institute, 194021 St. Petersburg, Russia
[3] Walter Schottky Institute, TU Munich, D-85748 Garching, Germany

ABSTRACT

The photogalvanic effects, which require a system lacking inversion symmetry, become possible in SiGe based quantum well (QW) structures due to their built-in asymmetry. We report on observations of the circular and linear photogalvanic effects induced by infrared radiation in (001)- and (113)-oriented $p-\mathrm{Si/Si}_{1-x}\mathrm{Ge}_x$ QW structures and analyse these observations in view of the possible symmetry of these structures. The circular photogalvanic effect arises due to optical spin orientation of free carriers in QWs with band splitting in **k**-space which results in a directed motion of free carriers in the plane of the QW. We discuss possible mechanisms that give rise to spin-splitting of the electronic subband states for different symmetries.

INTRODUCTION

The spin-degree of freedom of charge carriers and its manipulation has become a hot topic in material science under the perspective of spin-based electronic devices. One particular aspect, which we want to address in this contribution, is the generation of spin-polarized carriers in semiconductor quantum structures. This aspect is specific for the semiconductor material and can be considered without technological problems, like spin injection, inherent with the paradigmatic spin transistor proposed by Datta and Das [1]. Recently it has been demonstrated that in quantum well structures based on III-V compounds, a directed current inseparably linked to spin-polarized carriers can be created by circularly polarized light employing nonlinear optical properties [2,3]. This effect belongs to the class of photogalvanic effects known for bulk semiconductors [4].

The nonlinear optical response of matter under excitation by light with frequencies ω_1 and ω_2 is described in lowest order by a third rank tensor. The response is at the sum or difference frequency $\Omega = \omega_1 \pm \omega_2$. Special cases, with light from one intense light source ($\omega = \omega_1 = \omega_2$), are second harmonic generation ($\Omega = 2\omega$) and the photogalvanic effect ($\Omega = 0$). The latter is the generation of a direct current (double index summation understood)

$$j_\lambda = D_{\lambda\mu\nu} E_\mu(\omega) E_\nu(-\omega) \tag{1}$$

by applying light with the electric field amplitudes $E_\mu(t) = E_\mu(\omega)e^{i\omega t}$ and $E^*_\mu(\omega) = E_\mu(-\omega)$. For j_λ to be real one has $D_{\lambda\mu\nu} = D_{\lambda\nu\mu}$. Thus by decomposition of $D_{\lambda\mu\nu}$ into real and imaginary parts (being symmetric and antisymmetric, respectively, under interchange of the indices μ and ν) j_λ can be separated according to

$$j_\lambda = \chi_{\lambda\mu\nu} \left(E_\mu(\omega) E^*_\nu(\omega) + E^*_\mu(\omega) E_\nu(\omega) \right) / 2 + i\gamma_{\lambda\kappa} \left(\mathbf{E} \times \mathbf{E}^* \right)_\kappa , \tag{2}$$

where $\chi_{\lambda\mu\nu}$ is the real part of $D_{\lambda\mu\nu}$ and $\gamma_{\lambda\kappa}$ is a second-rank pseudo-tensor composed of the antisymmetric imaginary part of $D_{\lambda\mu\nu}$. The second term on the right-hand side of Eq. (2) can be expressed using $i(\mathbf{E} \times \mathbf{E}^*)_\kappa = \hat{e}_\kappa P_{circ} E_0^2$ with E_0 and $\hat{\mathbf{e}}$ being the electric field amplitude $|\mathbf{E}|$ and the unit vector pointing in the direction of light propagation, respectively. Because of the factor P_{circ}, indicating the degree of circular polarization, this term is identified with the circular photogalvanic effect (CPGE), while the first term of Eq. (2) contributes also for linearly polarized light and hence represents the linear photogalvanic effect (LPGE). Both effects require non-vanishing components of the tensor $D_{\lambda\mu\nu}$ which exist only in systems without a center of inversion, *i.e.* in bulk Si or Ge both effects are absent. However, in view of possible applications in spintronics based on SiGe it is

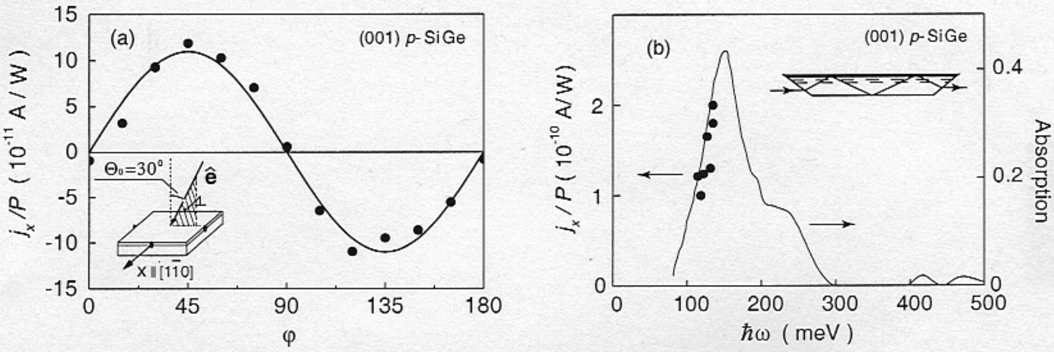

Figure 1. Photogalvanic current j_x in (001)-grown and asymmetrically doped SiGe QWs normalized by the light power P and measured at room temperature. (a) j_x/P as a function of the phase angle φ. The data were obtained under oblique incidence $\Theta_0 = 30°$ of irradiation at $\lambda = 10.6\,\mu$m. The full line is fitted after Eq. (3). (b) Spectral dependence of the CPGE (full dots) due to direct transitions between $hh1$ and $lh1$ valence subbands compared to the absorption spectrum obtained at 10 K from the transmission in a multiple-reflexion waveguide geometry shown in the inset.

important to note, that both effects become possible due to symmetry reduction in quantum well structures based on these materials. This is demonstrated by the experiments presented below where the inversion symmetry was broken by preparation of compositionally stepped quantum wells and asymmetric doping of compositionally symmetric quantum wells.

EXPERIMENT

The measurements were carried out on p-type SiGe quantum well structures MBE-grown on (001)- and (113)-oriented substrates. Two groups of (001)-grown samples were fabricated in the following manner. One of the groups of samples had a single quantum well of $Si_{0.75}Ge_{0.25}$ composition which was doped with boron from one side only. The second group comprised ten stepped quantum wells ($Si_{0.75}Ge_{0.25}$(4 nm)/ $Si_{0.55}Ge_{0.45}$(2.4 nm)), separated by 6 nm Si barriers. These structures are of C_{2v} point group symmetry which has also been confirmed by the present experiment. Structures of the lower symmetry C_s were (113)A-grown with a Si/$Si_{0.75}Ge_{0.25}$(5 nm)/Si single quantum well one-side boron doped. As a reference sample a (001)-grown compositionally symmetric and symmetrically boron doped multiple quantum well structure of sixty $Si_{0.7}Ge_{0.3}$(3 nm) quantum wells has been used.

All these samples had free carrier densities of about $8 \cdot 10^{11}\,cm^{-2}$ and were studied at room temperature. For (001)-oriented samples two pairs of ohmic point contacts in the center of the sample edges with connecting lines along $x \parallel [1\bar{1}0]$ and $y \parallel [110]$ have been prepared (see inset Fig. 1a). Two additional pairs of contacts have been formed in the corners of the samples corresponding to the $\langle 100 \rangle$-directions. For (113)-oriented samples two pairs of contacts were centered along opposite sample edges pointing in the directions $x \parallel [1\bar{1}0]$ and $y \parallel [33\bar{2}]$ (see inset in Fig. 2b).

A high power pulsed mid-infrared (MIR) TEA-CO_2 laser and a far-infrared (FIR) NH_3-laser have been used as radiation sources delivering 100 ns pulses with radiation power P up to 100 kW. Several lines of the CO_2 laser between 9.2 and 10.6 μm and of the NH_3-laser [5] between $\lambda = 76\,\mu$m and 280 μm have been used for excitation in the MIR and FIR range, respectively. The MIR radiation induces direct optical transitions between heavy hole and light hole subbands while the FIR radiation causes indirect optical transitions in the lowest heavy-hole subband. The laser light polarization was modified from linear to circular using for MIR light a Fresnel rhombus and for FIR radiation quartz $\lambda/4$ plates. The helicity of the incident light was varied according to $P_{circ} = \sin 2\varphi$ were φ is the angle between the initial plane of linear polarization and the optical axis of the $\lambda/4$

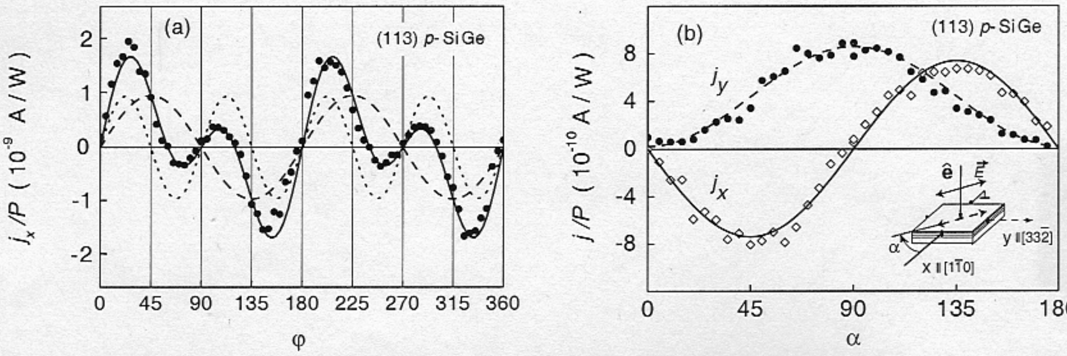

Figure 2. Photogalvanic current in (113)-grown SiGe QWs normalized by the light power P. The results were obtained under normal incidence of irradiation at $\lambda = 280\,\mu$m at room temperature. (a) Photocurrent j_x as a function of the phase angle φ. The full line is fitted after Eq. (6). Broken and dotted lines show $j_x \propto \sin 2\varphi$ and $j_x \propto \sin 2\varphi \cdot \cos 2\varphi$, respectively. (b) Photocurrent j in response to linear polarized radiation for x and y directions as a function of the angle α between the plane of linear polarization and the axis x. The broken line and the full line are fitted after Eq. (5).

plate. For investigation of the LPGE linearly polarized radiation has been used. In this case α is the angle between the electric field vector and the x direction (see inset in Fig. 2b).

With illumination by MIR radiation of the CO_2 laser in (001)-oriented samples with asymmetric quantum wells a current signal proportional to the helicity P_{circ} is observed under oblique incidence. We note that the samples were unbiased, thus the irradiated samples represent a current source. The current follows the temporal structure of the laser pulse intensity and changes sign if the circular polarization is switched from left to right handed (Fig. 1a). For $\langle 110 \rangle$ as well as $\langle 100 \rangle$ crystallographic directions the photocurrent flows perpendicular to the wavevector of the incident light. The wavelength dependence of the photocurrent obtained between 9.2 μm and 10.6 μm corresponds to the spectral behaviour of direct intersubband absorption between the lowest heavy hole and light hole subbands directly measured in transmission (see Fig. 1b).

In the FIR range a more complicated dependence of the current as function of helicity has been observed. In (001)-grown asymmetric quantum wells as well as in (113)-grown samples the observed dependence of the current on the phase angle φ may be described by the sum of two terms, one of them is $\propto \sin 2\varphi$ and the other $\propto \sin 2\varphi \cdot \cos 2\varphi$. In Fig. 2a experimental data and a fit to these functions are shown for a step bunched (113)-grown SiGe sample. For circularly polarized radiation ($\varphi = 45° + m \cdot 90°$, m is integer) the $\sin 2\varphi \cos 2\varphi$ term is equal to zero. This makes the assumption likely that this term is caused by the linear photogalvanic effect [2] with the electric field vector projected on the y-direction. In order to prove that, the photocurrent has been investigated in response to a linearly polarized radiation. Indeed the LPGE could be observed with the current along both the x and the y direction. Fig. 2b presents the measured dependence of j_x and j_y, as a function of the angle α between the plane of linear polarization and the axis x. The solid and the dashed curves in Fig. 2b show the fit after $j_x \propto \sin 2\alpha$ and $j_y \propto [\chi_+ - \chi_- \cos 2\alpha]$, respectively. Here χ_+ and χ_- are constants.

For both spectral ranges with (001)-grown samples a variation of the incidence angle Θ_0 in the incidence plane around Θ_0=0 changes the sign of the current. At normal incidence the current vanishes. This is observed for both the CPGE and the LPGE. For (113)-grown samples the current does not change its sign by the variation of Θ_0 and assumes its maximum at Θ_0=0.

In symmetrically (001)-grown and symmetrically doped SiGe quantum wells no photogalvanic current has been observed in spite of the fact that these samples, in order to increase their sensitivity, contain substantially more quantum wells than the asymmetric structure described above.

PHENOMENOLOGICAL DESCRIPTION

Several point groups are relevant in connection with the photogalvanic experiments using (001)- and (113)-oriented $Si/Si_{1-x}Ge_x$ QW structures on which we report here. We consider structures with ideal abrupt interfaces. The point symmetry of a single (001)-oriented hetero-interface between semiconductors with a diamond lattice is C_{2v} (the same as for zinc-blende hetero-interfaces). The symmetry of (001)-grown $Si/(Si_{1-x}Ge_x)_n/Si$ QWs depends on the number n of atomic layers forming the well. It is D_{2h} for even n and D_{2d} for odd n. In contrast to D_{2d} the point group D_{2h} has a center of inversion and thus forbids the second order response including both LPGE and CPGE as well as second-harmonic generation. An electric field (external or built-in) along the growth direction reduces the symmetry from D_{2h} or D_{2d} to C_{2v}. The point group C_{2v} includes the two-fold rotation axis $C_2 \parallel [001]$ and the mirror planes $\sigma_{(110)}, \sigma_{(1\bar{1}0)}$. In real (001)-grown QWs with monoatomic height-fluctuations like steps, islands, and terraces, the local C_{2v} symmetry increases to C_{4v} upon averaging over a certain in-plane area (see [6]). For symmetrical QWs with built-in electric fields or asymmetrical QWs (due to doping or different profiles of the left and right interfaces) the macroscopic symmetry is C_{2v} as for a single heterojunction. It should be noted here, that second harmonic generation has been detected in (001)-grown Si/SiGe QWs [7]. If an interface is grown along the low-symmetry axis $z \parallel [hhl]$ with $[hhl] \neq [001]$ or [111] the point group becomes C_s (see *e.g.* [8]) and contains only two elements, the identity and one mirror reflection plane $\sigma_{(1\bar{1}0)}$. Asymmetric (hhl)-grown QWs retain the point-group symmetry C_s and thus allow CPGE and LPGE as is the case for zinc-blende-based QWs grown on (113)-oriented substrates. The samples used in our experiments (see previous Section) have C_{2v} or C_s symmetry for (001)- or (113)-grown structures, respectively.

CPGE and LPGE depend in a characteristic way on the angular configuration of the experimental setup (see previous section). One angle (φ) is used to describe the changing polarization of the incident light between linear ($\varphi = 0, 90°, 180°, ..$) and circular ($\varphi = 45°, 135°, ..$), the second ($\alpha$) describes (for linear polarization) the angle between the plane of linear polarization and the x axis. Making use of the sample symmetry we derive these characteristic angular dependencies of the photocurrent j_λ of Eq. (2) on φ and α. In doing so we identify the coordinates x, y, z with the directions $[1\bar{1}0]$, $[ll(\overline{2h})]$ and $[hhl]$, respectively, where $[hhl]$ ([001] or [113] in our case) is the growth axis of the QW-structure. Due to carrier confinement in z direction the photocurrent in QWs has nonvanishing components only in x and y. Then, in a system of C_{2v} symmetry, the tensor γ describing the CPGE is characterized by two linearly independent components γ_{xy} and γ_{yx} and the second term of Eq. (2) reduces to

$$j_x = \gamma_{xy} \hat{e}_y P_{circ} E_0^2\,, \qquad j_y = \gamma_{yx} \hat{e}_x P_{circ} E_0^2 \tag{3}$$

with $P_{circ} = \sin 2\varphi$. A photocurrent can be induced in this case only under oblique incidence (as in Fig. 1a) because for normal incidence, $\hat{\mathbf{e}} = \boldsymbol{q}/q \parallel [001]$ and hence $\hat{e}_x = \hat{e}_y = 0$.

The C_s symmetry allows CPGE and LPGE for normal incidence $\hat{\mathbf{e}} \parallel [hhl]$ because in this case the tensors $\boldsymbol{\gamma}$ and $\boldsymbol{\chi}$ have the additional nonzero components γ_{xz}, $\chi_{xxy} = \chi_{xyx}$, χ_{yxx} and χ_{yyy}. As a result, under normally incident excitation, one has

$$j_x = \gamma_{xz} P_{circ} E_0^2 + \chi_{xxy}(E_x E_y^* + E_y E_x^*)\,, \qquad j_y = \chi_{yxx}|E_x|^2 + \chi_{yyy}|E_y|^2\,, \tag{4}$$

where $E_0^2 = |E_x|^2 + |E_y|^2$. In particular, for linearly polarized light one has

$$j_x = E_0^2 \chi_{xxy} \sin 2\alpha\,, \qquad j_y = E_0^2(\chi_+ + \chi_- \cos 2\alpha)\,, \tag{5}$$

where $\chi_\pm = (\chi_{yxx} \pm \chi_{yyy})/2$. In the experimental set-up where the laser light is linearly polarized along x and a $\lambda/4$ plate is placed between the laser and the sample, Eqs. (4) reduce to

$$j_x = E_0^2\,(\gamma_{xz} + \chi_{xxy}\cos 2\varphi)\sin 2\varphi\,, \qquad j_y = E_0^2\,(\chi_+ + \chi_- \cos 2\varphi)\;. \tag{6}$$

The dependencies of Eqs. (3), (5) and (6) have been observed in different SiGe QWs and are shown in Figs. 1a and 2.

MICROSCOPICAL THEORY

The principal microscopic aspect of a photon helicity driven current is the removal of spin-degeneracy in the subband states due to the reduced symmetry of the quantum well structure [3, 9]. It is related to the appearance of **k**-linear terms in the Hamiltonian,

$$H^{(1)} = \beta_{lm}\sigma_l k_m \tag{7}$$

where the real coefficients β_{lm} form a pseudo-tensor subjected to the same symmetry restrictions as γ and the σ_l are Pauli spin matrices. Below several scenarios will be presented which could contribute to β_{lm} in SiGe QWs with symmetries C_{2v} or C_s. As discussed in [3] the coupling between the carrier spin (σ_l) and momentum (k_m) together with the spin-controlled dipole selection rules yields a net current under circularly polarized excitation. Depending on the photon energy this spin photocurrent can be either due to direct or indirect intersubband transitions. The former (latter) is realized in our experiments presented in Fig. 1 (Fig. 2).

Spin degeneracy results from the simultaneous presence of time-reversal and spacial inversion symmetry. If one of these symmetries is broken the spin degeneracy is lifted. In our SiGe QW systems the spacial inversion symmetry is broken (the point groups C_{2v} and C_s do not contain the inversion operation) and, as a consequence, spin-dependent and **k**-linear terms appearing in the electron Hamiltonian lead to a splitting of the electronic subbands at finite in-plane wave vector. Microscopically different mechanisms can lead to **k**-linear terms, which will be discussed here briefly.

In the context of spin related phenomena in QW structures most frequently the so-called Rashba term [10] is taken into account. It is a prototype spin-orbit coupling term of the form $\alpha(\nabla V \times \mathbf{p})\cdot\boldsymbol{\sigma}$, where $\mathbf{p}$ is the momentum of the particle moving in the potential V and $\boldsymbol{\sigma}$ is the vector of the Pauli spin matrices. The weighting factor α depends on the material in which the QW structure, giving rise to the potential V, is realized. The Rashba term has axial symmetry and can exist as well in systems invariant under C_{2v} and C_s. ∇V can be identified with the electric field due to the (asymmetric) confinement and is parallel to the growth direction of the QW structure. In the context of $\mathbf{k}\cdot\mathbf{p}$ theory the Rashba term can be understood as resulting from the couplings between conduction and valence band states mediated by the momentum operator ($\mathbf{k}\cdot\mathbf{p}$-coupling) and the space coordinate z in the electric field term $V = eFz$. The Rashba term has the form $\sigma_x k_y - \sigma_y k_x$ and leads to a **k**-linear contribution to the subband dispersion. For hole states it has been discussed in [11].

Invoking the theory of invariants [12], the Hamiltonian acting in the twofold space of spin -1/2 particles can be represented in terms of 4 independent 2×2 matrices (the unit matrix and the Pauli spin matrices). In addition to the Rashba term (which has this form) there could be similar expressions but with higher powers of the wave vector (or the electric field). The 4×4 Hamiltonian for holes, usually described in the basis of angular momentum eigenstates with $J = 3/2$, $M = \pm 3/2$, $\pm 1/2$, requires for its most general form 16 independent matrices formed from angular momentum matrices J_x, J_y, J_z, their powers and products. Thus in combination with tensor operators, composed of components of the momentum (or wave vector) and the electric field, new terms are possible under C_{2v} and C_s. Some of these, which can be regarded as generalized Rashba terms, give rise to **k**-linear contributions in the hole subbands. The 4×4-Luttinger Hamiltonian, describing the valence band dispersion of bulk Si or Ge close to the center of the Brillouin zone, can be split into a spherical symmetric part (giving rise to an isotropic dispersion of spin degenerate bands) and an anisotropic term causing warping of these bands. In (hhl)-grown QWs with symmetry C_s the spherical part leads to a subband Hamiltonian, which includes heavy-light hole coupling even at zero in-plane wave vector (angular momentum M ceases to be a good quantum number under C_s). In addition the warping term mediates also a coupling between light and heavy hole states. Combining these two couplings, that derive from the Luttinger Hamiltonian, yields terms of the form $J_z k_x$. These terms are invariants under C_s and result in a spin-splitting of the hole subbands.

Finally we mention a mechanism to create **k**-linear terms and spin-splitting which comes from the C_{2v} symmetry of a (001)-grown SiGe interface and gives rise to coupling between heavy and light hole states [13]. The mixing may be described by the coupling Hamiltonian

$$H_{l\text{-}h} = \frac{\hbar^2}{m_0 a_0 \sqrt{3}} t_{l\text{-}h} \{J_x, J_y\} \delta(z - z_{if}) \,. \tag{8}$$

Here $\{J_x, J_y\}$ is the symmetrized product of angular momentum matrices with $J = 3/2$, z_{if} is the interface coordinate along the growth axis, m_0 the free electron mass, a_0 the lattice constant, and $t_{l\text{-}h}$ a dimensionless coupling coefficient. Note that a shift of the interface by one atomic layer interchanges the role of the axes $[1\bar{1}0]$ and $[110]$, which as a consequence, leads to a sign change of $t_{l\text{-}h}$ reversing the current. This heavy-light hole coupling in combination with that one inherent in the Luttinger Hamiltonian for QWs leads again to spin-dependent $\mathbf{k}$-linear terms.

CONCLUSIONS

In our experiments, carried out for different p-doped QW structures based on the SiGe material system we have demonstrated the possiblity to create a photon helicity driven stationary current due to the circular photogalvanic effect. Our experiments show the characteristic angular dependencies derived from the phenomenological formulation of the linear and circular photogalvanic effect. The experiments have been performed in different energy regimes allowing for direct and indirect intersubband transitions. We analyze the symmetry of the QWs under investigation and present different scenarios that can lead to spin-dependent $\mathbf{k}$-linear terms in the hole subband Hamiltonian, which are prerequisite for the appearance of the observed photocurrent. Our results provide the important information that spin-related phenomena, which so far have been considered to be specific for QW strucures based on zinc-blende materials, exist also in the SiGe QW systems. Saturation of the photogalvanic effects in our samples, on which we report separately, can be used to measure the spin-relaxation times in these systems.

ACKNOWLEDGEMENTS

Financial support from the DFG, the RFFI, the Russian Ministry of Sci. and the NATO linkage program is gratefully acknowledge.

REFERENCES

1. S. Datta and B. Das, *Appl. Phys. Lett.* **56**, 665 (1990).
2. S.D. Ganichev, H. Ketterl, W. Prettl, E.L. Ivchenko, and L.E. Vorobjev, *Appl. Phys. Lett.* **77**, 3146 (2000).
3. S.D. Ganichev, E.L. Ivchenko, S.N. Danilov, J. Eroms, W. Wegscheider, D. Weiss, and W. Prettl, *Phys. Rev. Lett.* **86**, 4358 (2001).
4. E.L. Ivchenko and G.E. Pikus, *Superlattices and Other Heterostructures. Symmetry and Optical Phenomena*, Springer Series in Solid State Sciences, vol. 110, Springer-Verlag, 1995; second edition 1997; Ch. 10.
5. S.D. Ganichev, *Physica B* **273-274**, 737 (1999).
6. D.J. Bottomley, H.M. Van Driel, and J.-M. Baribeau, (Proc. 22nd ICPS, World Scientific, Singapore, 1994) pp. 1572.
7. M. Seto, M. Helm, Z. Moussa, P. Boucaud, F.H. Julien, J.M. Lourtioz, J.F. Nützel, and G. Abstreiter, *Appl. Phys. Lett.* **65**, 2969 (1994).
8. D.J. Bottomley, H. Omi, and T. Ogino, *J. Crysal Growth* **225**, 16 (2001).
9. S.D. Ganichev, E. L. Ivchenko, and W. Prettl, *Physica E*, in press
10. Yu.L. Bychkov and E.I. Rashba, *J. Phys. C* **17**, 6039 (1984).
11. R. Winkler, *Phys. Rev. B* **62**, 4245 (2000).
12. G.L. Bir and G.E. Pikus, *Symmetry and Strain-induced Effects in Semiconductors* (Wiley, New York 1974).
13. E.L. Ivchenko, A.Yu. Kaminski, and U. Rössler, *Phys. Rev. B* **54**, 5852 (1996).